doi:10.1006/jmbi.2001.5006 available online at http://www.idealibrary.com on IDEAL® *J. Mol. Biol.* (2001) **312**, 865–873

JMB

Dynamic Regimes and Correlated Structural Dynamics in Native and Denatured Alpha-lactalbumin

Zimei Bu[1]*, Jeremy Cook[1,2] and David J. E. Callaway[3]

[1]*NIST Center for Neutron Research, National Institute of Standards and Technology Gaithersburg, MD 20899-8562, USA*

[2]*University of Maryland College Park, MD 20742, USA*

[3]*Picower Institute for Medical Research, Manhasset NY 11030-3849, USA*

**Corresponding author*

Understanding the mechanisms of protein folding requires knowledge of both the energy landscape and the structural dynamics of a protein. We report a neutron-scattering study of the nanosecond and picosecond dynamics of native and the denatured α-lactalbumin. The quasielastic scattering intensity shows that there are α-helical structure and tertiary-like side-chain interactions fluctuating on sub-nanosecond time-scales under extremely denaturing conditions and even in the absence of disulfide bonds. Based on the length-scale dependence of the decay rate of the measured correlation functions, the nanosecond dynamics of the native and the variously denatured proteins have three dynamic regimes. When $0.05 < Q < 0.5$ Å^{-1} (where the scattering vector, Q, is inversely proportional to the length-scale), the decay rate, Γ, shows a power law relationship, $\Gamma \propto Q^{2.42 \pm 0.08}$, that is analogous to the dynamic behavior of a random coil. However, when $0.5 < Q < 1.0$ Å^{-1}, the decay rate exhibits a $\Gamma \propto Q^{1.0 \pm 0.2}$ relationship. The effective diffusion constant of the protein decreases with increasing Q, a striking dynamic behavior that is not found in any chain-like macromolecule. We suggest that this unusual dynamics is due to the presence of a strongly attractive force and collective conformational fluctuations in both the native and the denatured states of the protein. Above $Q > 1.0$ Å^{-1} is a regime that displays the local dynamic behavior of individual residues, $\Gamma \propto Q^{1.8 \pm 0.3}$. The picosecond time-scale dynamics shows that the potential barrier to side-chain proton jump motion is reduced in the molten globule and in the denatured proteins when compared to that of the native protein. Our results provide a dynamic view of the native-like topology established in the early stages of protein folding.

Keywords: protein folding; protein folding dynamics; diffusion; neutron scattering; molten globule

Introduction

Proteins have the remarkable ability to fold accurately and quickly for biological activities. Understanding the mechanisms of protein folding remains an important task in biology. The rate of protein folding is determined by both the energy landscape and by the protein dynamics.[1–7] While the energy landscape of protein folding has been a subject of intense study, little is known experimentally about the dynamic behavior of an unfolded protein.

During the protein-folding process, a polypeptide chain can form partially folded intermediate states to avoid searching a large conformation space on the energy landscape. Learning the structural characteristics of the partially folded intermediate can help us to elucidate how proteins fold.[8] The protein-folding intermediates are considered to be heterogeneous.[9,10] However, whether protein tertiary contacts occur along with the secondary structures in the early stage of protein folding remains undetermined.[11–13] Protein folding *in vivo* may be quite different from *in vitro*, since a polypeptide may fold co-translationally and protein folding *in vivo* sometimes needs the assistance of molecular chaperones. Studying the structural dynamics of a denatured protein can help us learn the physics and chemistry principles that govern protein folding.

Abbreviations used: QENS, quasielastic neutron-scattering; Q, scattering vector; Γ, decay rate; D_{eff}, effective diffusion constant.

E-mail address of the corresponding author: zimei.bu@nist.gov

0022-2836/01/040865–9 $35.00/0

Because of the importance of knowing both the structure and the dynamics in understanding protein folding, we have used quasielastic neutron-scattering (QENS) to study protein-folding dynamics. In a QENS experiment, the scattering intensity is a function of both the scattering vector, Q, and the neutron energy transfer, ΔE, caused by the density fluctuation of the measured molecules. Here $Q = 4\pi\sin\theta/\lambda$, where 2θ is the scattering angle and λ the wavelength, and $\Delta E = \hbar\omega$ where $\hbar$ is the Planck constant and ω the angular frequency of the neutrons. QENS therefore measures the scattering vector-dependent decay rate of the density fluctuations correlation function on picosecond to nanosecond time-scales.[14] Additionally, like static large-angle diffuse X-ray or neutron-scattering experiments on proteins in solution,[15] QENS can also probe changes in the correlation maxima corresponding to the secondary and tertiary structural changes of a protein. Dynamic as well as structural information of a protein can therefore be extracted from a QENS experiment.

We have reported a QENS study on the picosecond dynamics of the native and the molten globule of α-lactalbumin, and have found that the potential barrier to side-chain torsional motion is reduced in the molten globules.[16] Here, we use QENS to study the nanosecond and the picosecond dynamics of native and variously denatured states of α-lactalbumin. We show that the nanosecond dynamics of α-lactalbumin has three dynamic regimes on the length scale of $0.05 < Q < 1.75$ Å^{-1} studied by QENS. For scattering vector values $0.05 < Q < 0.5$ Å^{-1}, the characteristic decay rate Γ of the density correlation function follows a power law relationship $\Gamma \propto Q^{2.42 \pm 0.08}$ that is close to the $\Gamma \propto Q^3$ power law relationship found in polymer-chain dynamics.[17,18] However, at $0.5 < Q < 1.0$ Å^{-1}, in contrast to a polymer chain, Γ of both the native protein and the denatured states follows a $\Gamma \propto Q^{1.0 \pm 0.2}$ power law relationship. The effective diffusion constant $\Gamma/\hbar Q^2$ decreases with increasing Q. This unusual dynamics behavior indicates the existence of a new dynamic regime in denatured proteins that has lower conformational entropy than does a polymer random coil. There are also correlated conformational fluctuations in a protein even under extremely denaturing conditions. Additionally, the quasielastic intensity demonstrates the coexistence of secondary and tertiary structural fluctuations in highly denatured states of α-lactalbumin with the disulfide bonds reduced. Our results reveal that native-like topology exists in highly denatured α-lactalbumin. Because of the presence of such strong interactions, the dynamics of denatured proteins distinguish themselves from the dynamics of ordinary polymers.

The small, calcium-binding protein α-lactalbumin represents a class of proteins that can form partially folded intermediates, the so-called molten globules.[19] Native α-lactalbumin has two domains (see Figure 1), the α-domain (consisting largely of α-helices), and the β-domain (which has a significant β-sheet content).[20] α-Lactalbumin also has four disulfide bonds, two in the α-domain, one in the β-domain and one cross-linking the two domains. The structure of the α-lactalbumin molten globule is highly heterogeneous, having a structured α-domain with some native-like packing interactions, but an unstructured β-domain and loop regions.[21–24] The denatured states of α-lactalbumin are also heterogeneous. From NMR equilibrium studies, Schulman *et al.*[25] have shown that the unfolding of a α-lactalbumin molten globule is non-cooperative, and that the α-domain remains a collapsed core in the denatured states.

Figure 1. The structure of native α-lactalbumin. There are four disulfide bonds. The calcium ion is located in the helix-turn-helix motif that spans the interface between the α and the β-domains.

Recently Portman *et al.*[7] have developed a folding rate theory by analyzing the microscopic dynamics of chain motions. Portman *et al.* have extended the Rouse-Zimm formalism in polymer dynamics to incorporate chain internal friction arising from the isomerization of the backbone dihedral angles. The Rouse-Zimm model considers the conformational entropy as the source of restoring force for a random coil away from equilibrium. The folding rate of λ-repressor was calculated based on the Portman model. Possible contributions of residue-specific interactions to the complexity of protein folding dynamics are further acknowledged by Portman *et al.*,[7] who therefore consider the motion of an unfolded protein to be more restricted than that of a polymer chain.[7] It would be interesting to have a direct comparison of the neutron-scattering experimental results with the theoretical model on the same protein in the future.

Results

The nanosecond dynamics shows the presence of dynamic regimes and strongly correlated density fluctuations within the native protein and the denatured states

We have compared the QENS dynamics results of the native and the denatured α-lactalbumin to the dynamics of model polymer random coils. A brief review of the dynamics behaviors of a random coil is given here. It is established in polymer physics that the dynamics of a random coil has three regimes.[17,18] (1) When $QR_g < 1$, $\Gamma \propto Q^2$, as in the case of a freely diffusing particle, where R_g is the radius of gyration of the molecule. (2) When $QR_g > 1$, the chain dynamics follows the (Rouse-Zimm model): $\Gamma \propto Q^4$ (Rouse model) due to the polymer chain conformation entropy effect, and when long-range intramolecular interactions are absent.[26] Zimm has made a correction for a random coil with long-range hydrodynamic interactions in a dilute solution:[27] $\Gamma \propto Q^3$ (Zimm model).

The Rouse-Zimm model was later further improved to incorporate the barrier to bond torsional motion and chain rigidity or the intramolecular viscosity effects[28,29] to give a power exponent between 2 and 3.[30] (3) On even shorter length-scales when $Q_r \geqslant 1$ (r is the size of a residue), $\Gamma \propto Q^2$, is a dynamic regime that is characteristic of local dynamics of an individual residue without ''sensing'' the interactions with its nearest neighbors.[31]

Figure 2(a) and (b) show the neutron-scattering results. Figure 2(a) shows the nanosecond decay rate (Γ or $1/\tau$) of the density correlation function as a function of momentum transfer Q. There are three dynamic regimes in both the native protein and the unfolded proteins. In one regime, when $0.05 < Q < 0.5$ Å^{-1} (corresponding to $0.8 < QR_g < 8$ where R_g, the radius of gyration of the native α-lactalbumin, is equal to 16 Å), a power-law relationship $\Gamma \propto Q^{2.42 \pm 0.08}$ is found. This result is analogous to the dynamics of a rigid polymer chain with internal viscosity when $QR_g > 1$.[17,30]

However, when $0.5 < Q < 1.0$ Å^{-1} (corresponding to $8 < QR_g < 16$), a power-law relationship $\Gamma \propto Q^{1.0 \pm 0.2}$ is obtained (see Figure 2(a)), signifying a new dynamic behavior that is different from that of any chain-like polymers. This unusual dynamics behavior can also be viewed from the Q dependence of the effective diffusion constant, $D_{eff} = \Gamma/\hbar Q^2$ (see Figure 2(b)). The effective diffusion constant, D_{eff}, first increases with Q in the region of $0.25 < Q < 0.5$ Å^{-1}, and then D_{eff} decreases with Q when $0.5 < Q < 1.0$ Å^{-1}.

A third dynamic regime appears at $Q > 1.0$ Å^{-1} (corresponding to $QR_g > 16$) where $\Gamma \propto Q^{1.8 \pm 0.3}$ indicating that the local dynamics of individual residues becomes apparent. In the region of $Q > 1.0$ Å^{-1}, D_{eff} becomes independent of Q. It is also interesting to point out that the native protein and the differently denatured proteins have the same magnitude of the decay rate, despite the changes in the overall dimension of the unfolded states and the increased viscosity at high denaturant concentrations (see Figure 2(a) and (b)).

The picosecond dynamics shows reduced potential barrier to side-chain torsional motion in the molten globule and in the denatured protein

Figure 3 shows the picosecond dynamic decay rate Γ_f (see Materials and Methods) *versus* Q. On picosecond time-scales, QENS determines proton jump motions. Since in a deuterium-exchanged protein the majority of the protons are on the hydrophobic side-chains, the rotational jump motion (or side-chain rotamer torsional motion) are mainly measured. Figure 3 shows that on longer length-scales of $Q < 1.0$ Å^{-1}, the side-chain protons undergo spatially restricted motion in the native protein, the molten globule and the denatured protein. The 9 M urea-denatured protein shows a less restricted long-range motion than the native protein and the molten globule, since the decay rate increases with Q, but the motion is still restricted, since the intercept of the decay rate Γ_f (or $1/\tau_f$) *versus* Q^2 cannot reach zero, as found in freely diffusive motion. On shorter length-scales of $Q > 1.0$ Å^{-1}, when dominated by local dynamics, the potential barrier to jump motion is reduced in the molten globule and in the denatured proteins. The above results on native α-lactalbumin and molten globules are also consistent with our previous picosecond QENS studies,[16] though an improved data fitting routine has been adopted in the present study by fitting the QENS spectra with two Lorentzian functions to seperate out the protein internal motion from the center-of-mass motion of the protein.

Tertiary-like side-chain interactions and residual helical secondary structures are both present in highly denatured α-lactalbumin

In static X-ray and neutron-scattering experiments on native proteins, secondary structure and tertiary side-chain packing interactions give rise to scattering maxima at defined scattering vector Q values that signify each structure. Helical secondary structures give a maximum at $Q_{max1} \approx 0.87$ Å^{-1}, corresponding to a Bragg distance of 7.2 Å.[15] Side-chain packing interactions generate a scattering maximum at $Q_{max2} \approx 1.32$ Å^{-1}, corresponding to a Bragg distance of about 4.7 Å. From large-angle X-ray scattering experiments and computational analysis on native globular proteins, the $Q_{max2} \approx 1.32$ Å^{-1} maximum has been shown to be caused mainly by the long-range side-chain packing interactions.[19,32,33]

Figure 4 is a 3D representation of the scattering intensity of α-lactalbumin as a function of both the

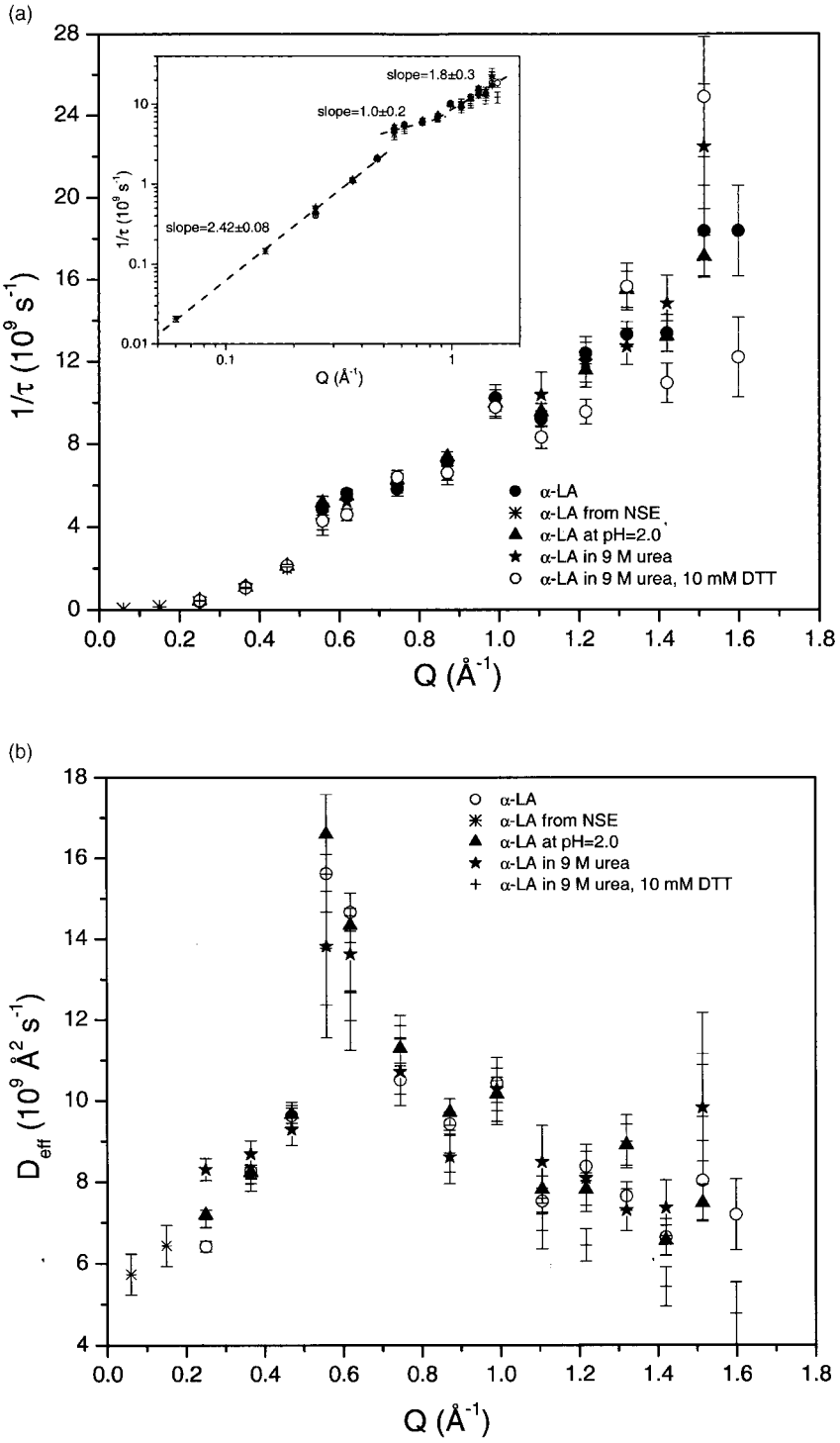

Figure 2. (a) The nanosecond decay rate ((or $1/\tau$) as a function of Q. (b) The effective diffusion constant $D_{\text{eff}} = \Gamma/\hbar Q^2$ of the native protein and the denatured proteins as a function of the scattering vector. Note that the two data points at $Q = 0.05$ and 0.16 Å^{-1} were collected on the new neutron spin-echo spectrometer at NIST and protein concentration effect on the reduction of diffusion constant was taken into account.

scattering vector, Q, and the neutron energy transfer, ΔE. The scattering intensity of the native protein shows two maxima, one at $Q_{\text{max1}} \approx 0.87$ Å^{-1} and another one at $Q_{\text{max2}} \approx 1.32$ Å^{-1} (see Figure 4(a)), indicating the presence of the helical structure and the side-chain packing interactions, respectively.

The two maxima do not disappear in the variously denatured α-lactalbumin samples as shown in Figure 4(b) to (d). Reducing the disulfide bonds

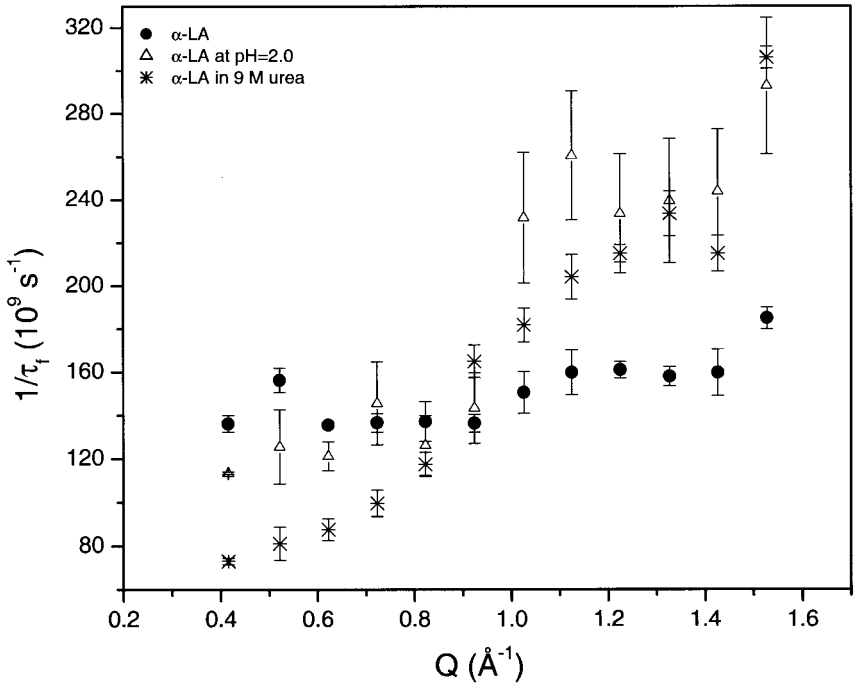

Figure 3. The picosecond decay rate Γ_f (or $1/\tau_f$) as a function of Q.

in 9 M urea with 10 mM DTT did not diminish the maxima either (see Figure 4(d)), suggesting the persistence of significant amount of helical structures and tertiary-like side-chain interactions under denaturing conditions with the disulfide bonds reduced. Since the measured dynamic range spans from about 3.8×10^{-11} to 1.3×10^{-9} second, the corresponding helical structure and the long-range

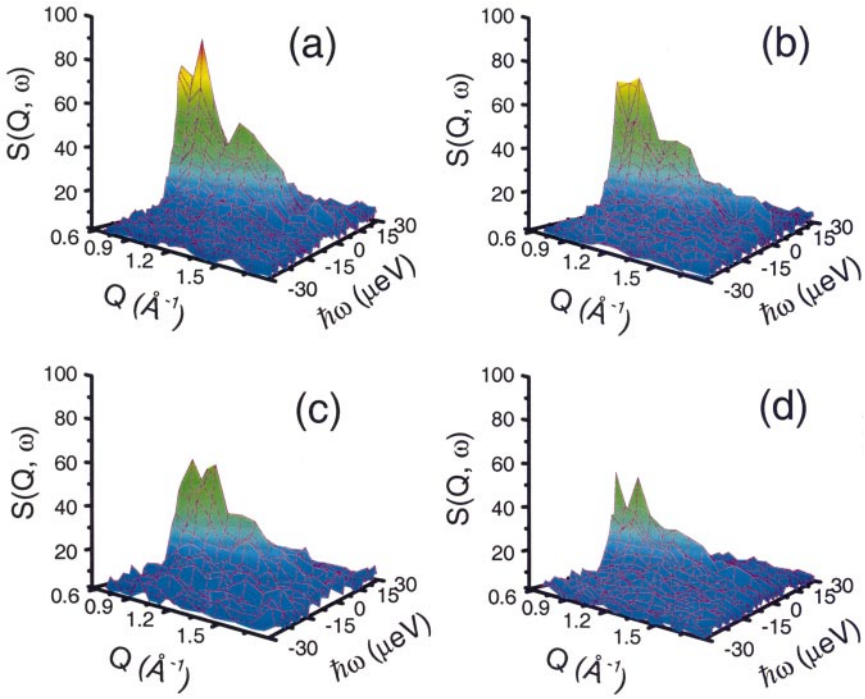

Figure 4. The 3D colored contour maps of the neutron-scattering intensity *versus* scattering vector Q and the energy transfer $\Delta E = \hbar\omega$ of the (a) native α-lactalbumin, (b) pH =2.0 molten globule, (c) α-lactalbumin in 9 M urea, and (d) α-lactalbumin in 9 M urea and 10 mM DTT. The dynamic range measured spans from 3.8×10^{-11} to 1.3×10^{-9} second.

side-chain interactions are fluctuating on several hundred picosecond time-scales (see Figure 2).

Discussion

The nanosecond QENS results show that a protein exhibits the dynamic behavior of normal polymer chains only on certain length-scales. In the case of α-lactalbumin, the Rouse-Zimm formalism is observed at $0.05 < Q < 0.5$ Å^{-1}, since $\Gamma \propto Q^{2.42 \pm 0.08}$; and at $Q > 1.0$ Å^{-1}, the local dynamics of a single residue (or bead) are demonstrated, since $\Gamma \propto Q^{1.8 \pm 0.3}$.

However, at $0.5 < Q < 1.0$ Å^{-1}, an unusual dynamics behavior is observed, since $\Gamma \propto Q^{1.0 \pm 0.2}$, or the effective diffusion constant decreases with increasing Q. The power law relationship of $\Gamma \propto Q^1$ found in a protein *versus* the $\Gamma \propto Q^3$ for random coils suggests that the conformational entropy is significantly lower in an unfolded protein than in a random coil. A decrease in the effective diffusion constant D_{eff} is a peculiar dynamic behavior that is not observed in chain-like polymers. This dynamic behavior is probably analogous to the ''interactive diffusion'' or collective density fluctuation phenomenon found in condensed atomic fluids and colloidal fluids upon melting,[34,35] due to the presence of attractive force and collective conformation fluctuations. Based on the QENS results, we suggest that there are correlated conformation fluctuations and strongly nonlocal, attractive forces within both the native and the denatured proteins.

The QENS intensity shows that there are fluctuating helical structure and long-range tertiary interactions in even highly denatured states, though the overall structure of the denatured states is disordered as evidenced by the expansion of the overall dimension of the protein upon denaturation and the reduced barriers to side-chain torsional motion as determined from the picosecond QENS. Both the residual secondary structure and tertiary-like long-range interactions are fluctuating over several hundred picoseconds in both the native protein and in the highly denatured states of α-lactalbumin.

The length-scale dependent decay rate of correlation function and the QENS scattering intensity demonstrate the presence of stronly correlated structure dynamics within the native protein, the molten globule, and the denatured α-lactalbumin. Highly correlated structural dynamics may be a universal intrinsic property of a polypeptide chain that has the ability to fold into a native protein. Collective dynamics and the presence of strongly attractive forces suggest that at least some regions of the denatured states are condensed. The QENS results are thus consistent with the findings that the molten globule of α-lactalbumin has a native-like tertiary topology,[23] and the residue-specific NMR study that finds α-lactalbumin has a collapsed core with structured α-helices under denaturing conditions.[25] The individual residues contributing to the native-like topology in α-lactalbumin molten globules have been identified to be mainly hydrophobic and in the α-domain.[36]

We have demonstrated the persistence of the residual helical structure and tertiary-like interactions even in the absence of disulfide bonds under highly denaturing conditions. There is evidence that a denatured protein can have ordered secondary and tertiary structures.[37–40] Under physiological conditions, an unfolded polypeptide chain may also be compact.[41] The QENS results on α-lactalbumin thus support the view that concurrent formation of secondary and tertiary structure clusters can occur in the early stages of protein folding.[10,42]

Materials and Methods

Materials

Native bovine α-lactalbumin and the acid form of molten globules at p^{2}H 2.0 for QENS experiments were prepared as described.[16] Denatured α-lactalbumin was prepared by dissolving deuterium-exchanged α-lactalbumin in 20 mM glycine-d_5, ^{2}HCl (p^{2}H 2.0), ^2H_2O in 9 M deuterated urea solution. The disulfide bond-reduced, denatured state was prepared by dissolving the protein in 9 M urea and 10 mM (1,4-dithio-D,L-threitol) DTT, 20 mM glycine-d_5, ^{2}HCl (p^{2}H 2.0) and ^2H_2O. Protein concentrations were 60 mg/ml for the native protein and about 15-20 mg/ml for the non-native states to avoid aggregations.

Quasielastic neutron-scattering experiment

Neutron-scattering experiments were conducted at the high flux backscattering spectrometer (HFBS) and the disc chopper spectrometer (DCS) of the National Institute of Standards and Technology Center for Neutron Research. The dynamic ranges (FWHM) of the instrument were 1-35 μeV on HFBS , and 32-1000 μeV on DCS. The scattering vector Q range varied from 0.25 to 1.75 Å^{-1} corresponding to a length-scale of 25.1-3.6 Å. The samples were loaded in a 0.8 mm thick Teflon-coated, aluminum annulus for measurements. Data collection times were about 24 hours on protein solutions and on the buffer background, respectively. Measurements were made at 30 °C. Background-subtraction and initial data treatments were performed as described.[16] The background-subtracted scattering intensity was normalized by protein concentration and the neutron counts from a beam monitor placed before the sample.

Neutron-scattering function and data analysis

The scattering intensity as a function of scattering vector and neutron energy transfer can be described by:[34]

$$I(Q, \omega) = S(Q)\frac{S'(Q, \omega)}{S(Q)} \quad (1)$$

where $S(Q)$ is the structure factor. From equation (1), it is apparent that the structural features $S(Q)$ of the measured sample, like a Bragg peak, can be shown in the Q dependence of quasielastic scattering intensity.

Table 1. The solvent viscosity, and the α-lactalbumin diffusion coefficient D_c and hydrodynamic radius R_h at 30 °C

	^2H_2O buffer	^2H_2O buffer at $p^2H = 2.0$	9 M urea in ^2H_2O	9 M urea, 10 mM DTT in ^2H_2O
Solvent viscosity η (cp)	1.3500	1.3500	2.0561	2.0561
α-Lactalbumin D_c (cm^2/s)	9.61×10^{-7}	8.05×10^{-7}	3.50×10^{-7}	1.00×10^{-7}
α-Lactalbumin R_h (Å)	17.1	20.4	30.8	107.8

$D_c = k_B T/6\pi\eta R_h$ where k_B is the Boltzmann constant, T is the temperature in Kelvin, η is the solvent viscosity.

The term:

$$S(Q, \omega) = \frac{S'(Q, \omega)}{S(Q)}$$

is the dynamic structure factor, i.e. the Fourier transform of the correlation function:[15]

$$S(Q, \omega) = \frac{1}{2\pi N} \int \langle \rho(0)_Q \rho(t)_Q \rangle \exp(-i\omega t) \mathrm{d}t \qquad (2)$$

Note that in equation (2), we do not attempt to determine if the dynamic structure factor arises from the coherent scattering or the incoherent scattering, since both have the same Γ *versus* Q relationship.[43]

The scattering spectra from the HFBS nanosecond dynamcis experiments were fit by a single Lorentzian function L(ω, Γ):

$$S(Q, \omega)_{HFBS} = \exp(-Q^2\langle u^2 \rangle/3) A(Q) L(\omega, \Gamma) \otimes R(Q, \omega)_{HFBS} + B_o + B_1\omega \qquad (3)$$

where the term $\exp(-Q^2\langle u^2 \rangle/3)$ is the Debye-Waller factor:

$$L(\omega, \Gamma) = \frac{1}{\pi} \frac{\Gamma}{\Gamma^2 + \omega^2}$$

is the Lorentzian function, with Γ being the half width at half maximum of the Lorentzian function, which is the characteristic decay rate of the correlation function. $A(Q)$ is the quasielastic intensity. $R(Q, \omega)_{HFBS}$ in equation (3) is the instrument resolution function that is convoluted with the quasielastic, Lorentzian function $L(\omega, \Gamma)$. $R(Q, \omega)_{HFBS}$ can be determined by measuring the scattering from vanadium, and $B_o + B_1\omega$ is the baseline.

The picosecond dynamics spectra collected from DCS were fit by two Lorentzian function $L_f(\omega, \Gamma_f)$ and $L_s(\omega, \Gamma_s)$, representing a slow mode of motion and a fast mode of motion, respectively:

$$S(Q, \omega)_{DCS} = \exp(-Q^2\langle u^2 \rangle/3) \times [A_f(Q) L_f(\omega, \Gamma_f) + A_s(Q) L_s(\omega, \Gamma_s)] \otimes R(Q, \omega)_{DCS} + B_o + B_1\omega \qquad (4)$$

where the term $\exp(-Q^2\langle u^2 \rangle/3)$ is the Debye-Waller factor and:

$$L_f(\omega, \Gamma_f) = \frac{1}{\pi} \frac{\Gamma_f}{\Gamma_f^2 + \omega^2}$$

and:

$$L_s(\omega, \Gamma_s) = \frac{1}{\pi} \frac{\Gamma_s}{\Gamma_s^2 + \omega^2}$$

are Lorentzian functions with Γ_f and Γ_s being the half width at half maximum of the Lorentzian functions. The decay rate Γ_f or $1/\tau_f$ of the fast mode represents the internal dynamics of the proteins, and the decay rate of the slow mode Γ_s or $1/\tau_s$ approxmately represents the center-of-mass diffusive motion of the protein. $A_f(Q)$ and $A_s(Q)$ are the quasielastic intensities of the fast mode and slow mode motion, respectively; $R(Q, \omega)_{DCS}$ is the instrument resolution functions that is convoluted with the quasielastic, Lorentzian functions $L_f(\omega, \Gamma_f)$ and $L_s(\omega, \Gamma_s)$, respectively; $B_o + B_1\omega$ is the baseline. $R(Q, \omega)_{DCS}$ can be determined by measuring the scattering from vanadium.

The results of the DCS time-of-flight data analysis methods described here are similar to what is described by Perez *et al.*,[44] though the two Lorentzian function fitting method developed in our study is straightforward and easy to implement experimentally. Note that although the $L_s(\omega, \Gamma_s)$ obtained from DCS is comparable to the $L(\omega, \Gamma)$ obtained from HFBS, the value of $L_s(\omega, \Gamma_s)$ was mostly below the DCS instrument resolution $R(Q, \omega)_{DCS}$ so that no information about the slow internal motion of the protein can be obtained from DCS or $L_s(\omega, \Gamma_s)$.

Dynamic light-scattering experiments

Dynamic light-scattering (DLS) experiments were performed to characterize the hydrodynamic radius of the native and the variously denatured α-lactalbumin samples in dilute protein solutions. The long length-scale decay rates obtained from DLS (of $Q = 0.00107$ $Å^{-1}$) can be used to estimate the center-of-mass diffusion of the proteins. DLS experiments were performed on a DynaPro-MS800 dynamic light-scattering instrument (Protein Solutions, Inc., Charlottesville, VA) at a fixed scattering angle of 90 ° and with the wavelength of the laser beam being 8324 Å. Proteins used in the DLS experiment were in ^2H_2O buffers like those used in the QENS experiments. DLS experiments were performed at 30.0 °C. The diffusion coefficients D_c and the calculated hydrodynamic radii R_h are listed in Table 1.

Acknowledgments

We thank D. A. Weitz, B. Nölting and J. X. Song for helpful discussions and communications; J. Copley and R. Dimeo for advice on the use of the DCS and HFBS instruments; Z. Chowdhuri for assistance with data collection; B. Hammouda, A. Senes for reading the manuscript. We acknowledge the National Institute of Standards and Technology, US Department of Commerce, for support and for providing the neutron facilities used in this work.

References

1. Bilsel, O. & Matthews, C. R. (2000). Barriers in protein folding reactions. *Advan. Protein Chem.* **53**, 153-207.
2. Bryngelson, J. D., Onuchic, J. N., Socci, N. D. & Wolynes, P. G. (1995). Funnels, pathways, and the energy landscape of protein folding: a synthesis. *Proteins: Struct. Funct. Genet.* **21**, 167-195.
3. Burton, R. E., Myers, J. K. & Oas, T. G. (1998). Protein folding dynamics: quantitative comparison between theory and experiment. *Biochemistry,* **37**, 5337-5343.
4. Chan, H. S. & Dill, K. A. (1998). Protein folding in the landscape perspective: chevron plots and non-Arrhenius kinetics. *Proteins: Struct. Funct. Genet.* **30**, 2-33.
5. Jacob, M. & Schmid, F. X. (1999). Protein folding as a diffusional process. *Biochemistry,* **38**, 13773-13779.
6. Karplus, M. & Weaver, D. L. (1994). Protein folding dynamics: the diffusion-collision model and experimental data. *Protein Sci.* **3**, 650-668.
7. Portman, J. J., Takada, S. & Wolynes, P. G. (2001). Microscopic theory of protein folding rates. II. Local reaction coordinates and chain dynamics. *J. Chem. Phys.* **114**, 5082-5096.
8. Dill, K. A. & Shortle, D. (1991). Denatured states of proteins. *Annu. Rev. Biochem.* **60**, 795-825.
9. Dobson, C. M. & Karplus, M. (1999). The fundamentals of protein folding: bringing together theory and experiment. *Curr. Opin. Struct. Biol.* **9**, 92-101.
10. Nolting, B. & Andert, K. (2000). Mechanism of protein folding. *Proteins: Struct. Funct. Genet.* **41**, 288-298.
11. Baldwin, R. L. & Rose, G. D. (1999). Is protein folding hierarchic? I. Local structure and peptide folding. *Trends Biochem. Sci.* **24**, 26-33.
12. Baldwin, R. L. & Rose, G. D. (1999). Is protein folding hierarchic? II. Folding intermediates and transition states. *Trends Biochem. Sci.* **24**, 77-83.
13. Fersht, A. R. (2000). Transition-state structure as a unifying basis in protein-folding mechanisms: contact order, chain topology, stability, and the extended nucleus mechanism. *Proc. Natl Acad. Sci. USA,* **97**, 1525-1529.
14. Bee, M. (1988). *Quasielastic Neutron Scattering, Principles and Applications in Solid State Chemistry, Biology and Materials Science*, Adam Hilger, Bristol and Philadelphia.
15. Glatter, O. & Kratky, O. (1982). *Small Angle X-ray Scattering*, Academic Press, London, New York.
16. Bu, Z., Neumann, D. A., Lee, S. H., Brown, C. M., Engelman, D. M. & Han, C. C. (2000). A view of dynamics changes in the molten globule-native folding step by quasielastic neutron scattering. *J. Mol. Biol.* **301**, 525-536.
17. Doi, M. & Edwards, S. F. (1986). *The Theory of Polymer Dynamics*, Clarendon Press, Oxford University Press, Oxford and New York.
18. de Gennes, P.-G. (1979). *Scaling Concepts in Polymer Physics*, Cornell University Press, Ithaca, NY.
19. Ptitsyn, O. B. (1995). Molten globule and protein folding. *Advan. Protein Chem.* **47**, 183-229.
20. Pike, A. C., Brew, K. & Acharya, K. R. (1996). Crystal structures of guinea-pig, goat and bovine alpha-lactalbumin highlight the enhanced conformational flexibility of regions that are significant for its action in lactose synthase. *Structure,* **4**, 691-703.
21. Alexandrescu, A. T., Ng, Y. L. & Dobson, C. M. (1994). Characterization of a trifluoroethanol-induced partially folded state of alpha-lactalbumin. *J. Mol. Biol.* **235**, 587-599.
22. Baum, J., Dobson, C. M., Evans, P. A. & Hanley, C. (1989). Characterization of a partly folded protein by NMR methods: studies on the molten globule state of guinea pig alpha-lactalbumin. *Biochemistry,* **28**, 7-13.
23. Peng, Z. Y., Wu, L. C., Schulman, B. A. & Kim, P. S. (1995). Does the molten globule have a native-like tertiary fold? *Phil. Trans. Roy. Soc. London ser. B,* **348**, 43-47.
24. Wu, L. C., Peng, Z. Y. & Kim, P. S. (1995). Bipartite structure of the alpha-lactalbumin molten globule. *Nature Struct. Biol.* **2**, 281-286.
25. Schulman, B. A., Kim, P. S., Dobson, C. M. & Redfield, C. (1997). A residue-specific NMR view of the non-cooperative unfolding of a molten globule. *Nature Struct. Biol.* **4**, 630-634.
26. Rouse, P. E. (1953). A theory of the linear viscoelastic properties of dilute solutions of coiling polymers. *J. Chem. Phys.* **21**, 1272-1280.
27. Zimm, B. H. (1956). Dynamics of polymer molecules in dilute solution: viscoelasticity, flow birefringence and dielectric loss. *J. Chem. Phys.* **24**, 269-278.
28. Allegra, G. & Ganazzoli, F. (1997). Polymer dynamics in solution - universal properties vs. individual behaviour in a unified approach. *J. Chem. Soc. Faraday Trans.* **93**, 2341-2353.
29. Fixman, M. (1988). Dynamics of stiff polymer-chains. *J. Chem. Phys.* **89**, 2442-2462.
30. Arbe, A., Monkenbusch, M., Stellbrink, J., Richter, D., Farago, B., Almdal, K. & Faust, R. (2001). Origin of internal viscosity effects in flexible polymers: a comparative neutron spin-echo and light scattering study on poly(dimethylsiloxane) and polyisobutylene. *Macromolecules,* **34**, 1281-1290.
31. Pecora, R. (1985). *Dynamic Light Scattering: Applications of Photon Correlation Spectroscopy*, Plenum Press, New York.
32. Fedorov, G. A. & Ptitsyn, O. B. (1977). Nature of the 4.5 Å maximum on curves of X-ray diffuse scattering of proteins and structured polypeptides. *Doklady Adademii Nauk SSSR,* **233**, 716-718.
33. Pickover, C. A. & Engelman, D. M. (1982). On the interpretation and prediction of X-ray scattering profiles from biomolecules in solution. *Biopolymers,* **21**, 817-831.
34. Balucani, U. & Zoppi, M. (1994). *Dynamics of the Liquid State. Oxford Series on Neutron Scattering in Condensed Matter* (Lovesey, S. W. & Mitchell, E. W. J., eds), Clarendon Press, Oxford.
35. Pusey, P. N. (1991). Colloidal suspensions. In *Liquids, Freezing and Glass Transition* (Hansen, J. P., Levesque, D. & Zinn-Justin, J., eds), pp. 763-942, North Holland, Amsterdam.
36. Song, J., Bai, P., Luo, L. & Peng, Z. Y. (1998). Contribution of individual residues to formation of the native-like tertiary topology in the alpha-lactalbumin molten globule. *J. Mol. Biol.* **280**, 167-174.
37. Kazmirski, S. L., Wong, K. B., Freund, S. M., Tan, Y. J., Fersht, A. R. & Daggett, V. (2001). Protein folding from a highly disordered denatured state: the folding pathway of chymotrypsin inhibitor 2 at atomic resolution. *Proc. Natl Acad. Sci. USA,* **98**, 4349-4354.
38. Sinclair, J. F. & Shortle, D. (1999). Analysis of long-range interactions in a model denatured state

of staphylococcal nuclease based on correlated changes in backbone dynamics. *Protein Sci.* **8**, 991-1000.
39. Yao, J., Chung, J., Eliezer, D., Wright, P. E. & Dyson, H. J. (2001). NMR structural and dynamic characterization of the acid-unfolded state of apomyoglobin provides insights into the early events in protein folding. *Biochemistry,* **40**, 3561-3571.
40. Rumbley, J., Hoang, L., Mayne, L. & Englander, S. W. (2001). An amino acid code for protein folding. *Proc. Natl Acad. Sci. USA,* **98**, 105-112.
41. Flanagan, J. M., Kataoka, M., Shortle, D. & Engelman, D. M. (1992). Truncated staphylococcal nuclease is compact but disordered. *Proc. Natl Acad. Sci. USA,* **89**, 748-752.
42. Fersht, A. R. (1995). Optimization of rates of protein folding: the nucleation-condensation mechanism and its implications. *Proc. Natl Acad. Sci. USA,* **92**, 10869-10873.
43. de Gennes, P. G. (1976). Dynamics of entangled polymer solutions. I. The rouse model. *Macromolecules,* **9**, 587-593.
44. Perez, J., Zanotti, J. M. & Durand, D. (1999). Evolution of the internal dynamics of two globular proteins from dry powder to solution. *Biophys. J.* **77**, 454-469.

Edited by M. F. Moody

(Received 11 May 2001; received in revised form 11 August 2001; accepted 13 August 2001)